

Protection of Carbon Steel against Hot Corrosion Using Thermal Spray Si- and Cr-Base Coatings

J. Porcayo-Calderon, J.G. Gonzalez-Rodriguez, and L. Martinez

(Submitted 18 July 1997; in revised form 26 September 1997)

A Fe75Si thermal spray coating was applied on the surface of a plain carbon steel baffle plate. Beneath this coating, a Ni20Cr coating was applied to give better adherence to the silicon coating. The baffle was installed in the high-temperature, fireside, corrosion zone of a steam generator. At the same time, an uncoated 304 stainless steel baffle was installed nearby for comparison. For 13 months the boiler burned heavy fuel oil with high contents of vanadium. The samples were studied employing scanning electron microscopy, x-ray microanalysis, and x-ray diffraction techniques. After that, it was possible to inspect the structural state of the components, and it was found that the stainless steel baffle plates were destroyed almost completely by corrosion, whereas the carbon steel coated baffle plate did not suffer a significant attack, showing that the performance of the thermal spray coating was outstanding and that the coating was not attacked by vanadium salts of the molten slag.

Keywords carbon steel, hot corrosion, Si-base coating, thermal spray

1. Introduction

High-temperature alloys must have good mechanical properties and corrosion resistance and be relatively easy to manufacture. However, it is not likely for a single alloy to have all these properties. Most high temperature alloys are iron-, nickel-, or cobalt-base because these elements have high melting points and are easy to manufacture without problems. Unfortunately, their oxides are not protective enough in the combustion environment of a fossil-fuel power plant at temperatures above 550 °C. Nevertheless, addition of other elements to establish more protective oxides such as Cr₂O₃, Al₂O₃, or SiO₂ has improved their corrosion resistance. These oxides offer protection due to their low growth rate and the effective barrier they provide against ionic migration (Ref 1-3).

The threshold amount required in the alloy for the establishment of a continuous protective oxide layer depends on the alloying elements. Chromium affects the mechanical properties of the alloys the least, but a higher threshold value is required to allow a passive behavior against oxidation (16 to 20%). For aluminum additions, a threshold value of 15% is required (Ref 1, 2), whereas for silicon additions to steel the threshold value is the lowest, 5% (Ref 2, 4, 5).

Although the addition of aluminum or silicon gives alloys the best oxidation and corrosion resistance because they form protective oxides with low growth rate, their incorporation can affect the mechanical properties of the alloy. It has been observed that a third element, normally chromium, which forms

an oxide with a stability between the one for the base metal oxide and the one for the protective element (aluminum or silicon), enhances the formation of a protective scale with lower amounts of aluminum or silicon (Ref 1, 2, 6, 7). In the case of Fe-Cr-Si alloys, Robertson et al. attribute this to a synergistic effect between chromium and silicon where chromium acts as a secondary getter, lowering the oxygen solubility in the metal and thus the silicon required to form the protective layer (Ref 7), but this mechanism is still open to speculation.

The effectiveness of a protective oxide scale depends on several factors, and it must be free of stoichiometric imperfections, porosity, cracks, and stresses and be resistant to descaling and stable in service. Unfortunately, it is almost impossible to develop such scales because they are susceptible to fail either by fracture or by descaling at high temperature. In some situations, the alloy can be reheated and the protection is kept. However, if the chromium, aluminum, or silicon contents are depleted, then oxides from the base metal can be formed, although they are less protective, accelerating the degradation process (Ref 1).

It is obvious that adding large amounts of alloying elements to form protective oxides ensures that the formation of a continuous layer of a protective oxide and a reservoir that enhances the formation of such scales are maintained; however, such additions will drastically lower the mechanical properties of the alloy. Thus, a way to incorporate large amounts of alloying elements to form protective oxides is applying it as a coating in such a way that the mechanical properties of the alloy are kept. Generally, two types of coating processes can be distinguished: one requires that the surface composition be altered by diffu-

Table 1 Chemical analysis of the carbon and steel plates

Element	Composition, wt%
Silicon	0.25
Carbon	0.54
Nickel	0.02
Phosphorus	0.001
Manganese	1.75
Sulfur	0.035
Iron	bal

J. Porcayo-Calderon, Instituto de Investigaciones Electricas, Sistemas de Combustion, Interior Internado Palmira, Apdo. Postal 1-475, 62000-Cuernavaca, Mor., Mexico; **J.G. Gonzalez-Rodriguez**, U.A.E.M., Facultad de Ciencias Quimicas e Ingenieria, Av. Universidad 1001, Cuernavaca, Mor., Mexico; and **L. Martinez**, Instituto de Fisica, UNAM, Laboratorio Cuernavaca, Apdo. Postal 48-3, 62251-Cuernavaca, Mor., Mexico.

sion and the other involves the deposition of a metallic or ceramic overlay with improved oxidation resistance (Ref 8).

Even when it has been shown that iron-silicon alloys have excellent corrosion and oxidation resistance (Ref 1, 2, 5-7), little attention has been paid to this system in a protective coating application (Ref 9). Most silicon coatings are ceramic-based, such as SiC, Si₃N₄, zirconium-silicon, and titanium-silicon, or enriching the surface with silicon or applying it as SiO₂. Some of the employed techniques involve chemical vapor deposition, pack cementation, plasma spraying, electron beam evaporation, ion plating, sputtering, and laser fusion (Ref 10-19).

Corrosion of materials exposed to combustion gases in boilers that use heavy fuel oil is a severe problem that affects their reliability. Particularly, it has been reported that materials normally used in superheaters and reheaters in Mexican boilers are highly sensitive to high-temperature corrosion enhanced by liquid phase fuel oil ash deposits (Ref 20). Components of the superheaters and reheaters such as spacers, deflective baffles,

and bracers, which are not water cooled, work at temperatures near those of the combustion gases. This, together with high contents of vanadium, sodium, and sulfur in the fuel, particular operational procedures, and boiler design, causes high corrosion rates in these components (Ref 21).

A previous paper (Ref 9) discussed the high corrosion resistance of the iron-silicon system used to coat a 304-H additive feeder in vanadium compound environments. In this work, a carbon steel baffle that normally exhibited catastrophic corrosion rates installed in the secondary reheater of a 350 MW boiler was coated with iron-silicon coating using the thermal spray technique.

2. Materials and Experimental Procedure

The baffles were installed in the secondary reheater of a 350 MW boiler, where the temperature of the combustion gases was

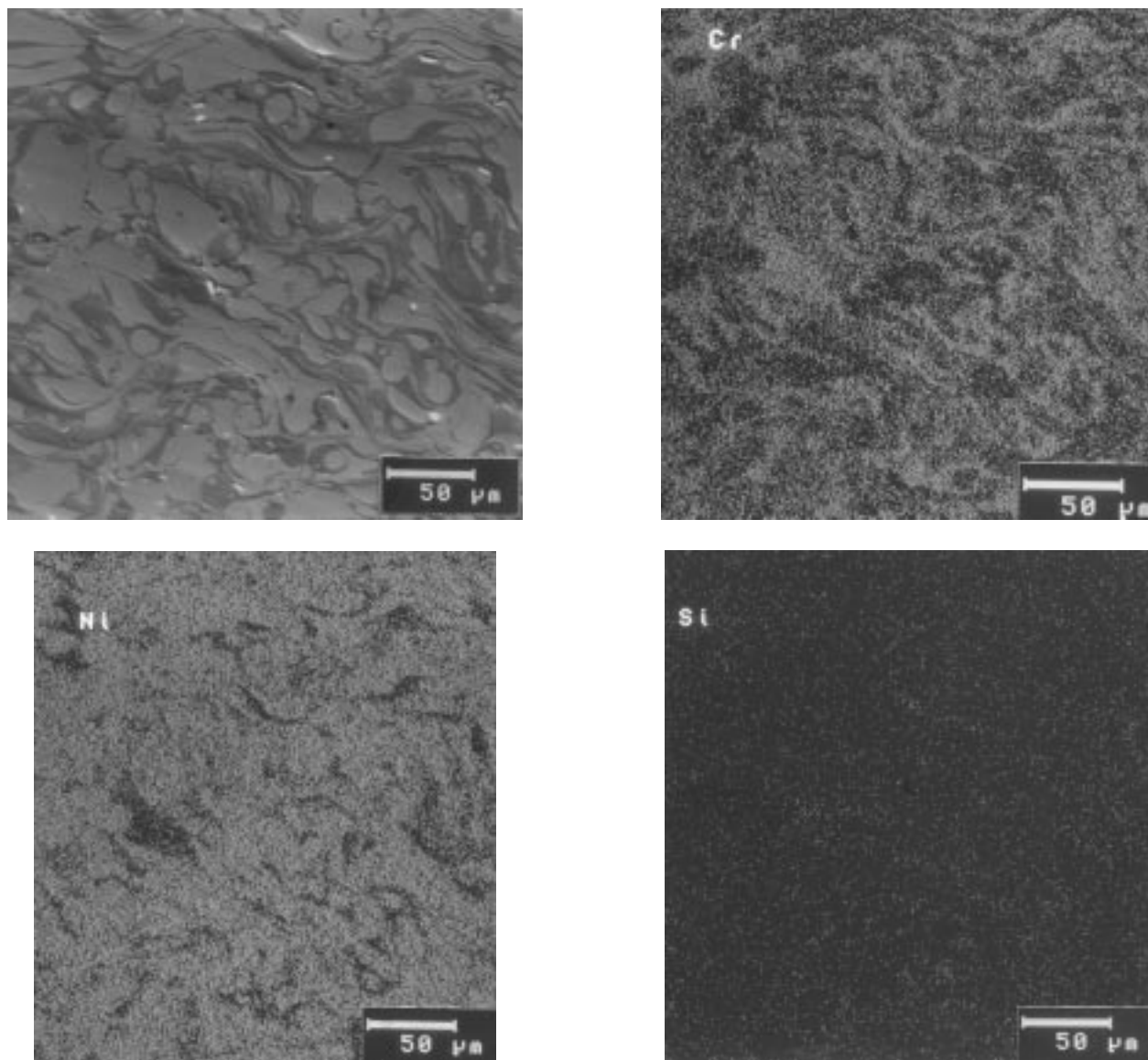


Fig. 1 Secondary electron image of the cross section for the as-deposited Ni20Cr coating and the elements present (Cr, Ni, and Si)

around 830 °C (Ref 22) and slags had accumulated on the tube surfaces.

The deflective baffles (not water cooled) in this part of the boiler were made of 304 type stainless steel, which within 6

months suffered from rather high corrosion rates and practically disappeared within a period of 12 months. These baffles were formed with five plates 5 mm thick and 650 mm wide, and when they were all together, the baffle was 8 m long. According

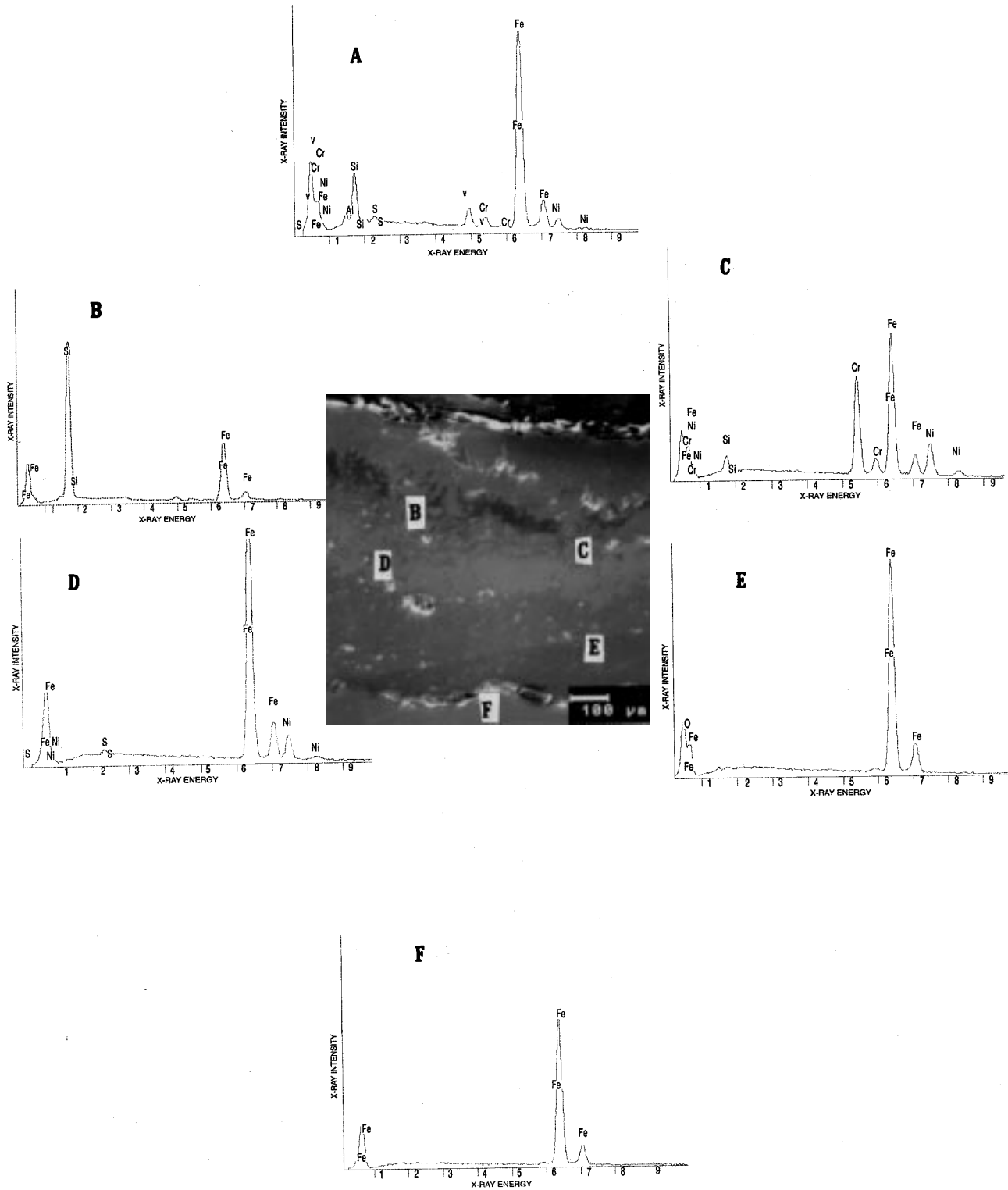


Fig. 2 Secondary electron image of the Fe75Si-Ni20Cr coating system and the base metal together with EDX spectra of the identified zones. (a) External deposit. (b) Silicon-base coating. (c) Ni20Cr coating. (d) Nickel-rich base metal. (e) Internal oxidized zone. (f) Base metal

to these data, it can be said that the average corrosion rate was, at least, 5 mm/yr.

For this work, the baffle was made of carbon steel, the chemical composition of which is shown in Table 1, and it was coated with a two-layer coating system. For comparison, some baffles were made of 304 type stainless steel and placed in the same part.

The two-layer coating system consisted of a Ni20Cr-base coating, around 100 μm thick, which had a bonding effect, and the silicon-base coating was applied over it. Table 2 shows the chemical composition of both coatings.

The coatings were applied using a powder flame spraying gun using a mixture of oxygen and acetylene as the heat source. Prior to the application of the coating, the carbon steel plates were sandblasted to eliminate impurity and oxides and then sandblasted with metallic grit to obtain a rough surface. After this, the plates were degreased with a solvent and preheated at

100 to 120 $^{\circ}\text{C}$. In these conditions the plates were ready for the coatings—first the Ni20Cr-base coating until a thickness of 100 μm had been reached, and then the silicon-base coating, applied to the same thickness.

Figure 1 shows a cross section of the as-deposited Ni20Cr-base coating. Silicon is dispersed throughout the material. The characteristics of the coating are typical of the coatings applied with this technique, that is, the presence of flakes with round partially melted particles.

It was observed that the silicon-base coating had low adherence in its particles and high porosity, and this made it impossible to prepare a metallographic sample to be observed in a scanning electron microscope (SEM). For this reason, once the coatings were applied an aluminum-base sealer was applied to close the porosity. The exposure time was 13 months (9360 h), during which the boiler was working at maximum load of 350 MW through the day and at low loads, in the range of 200 to 300

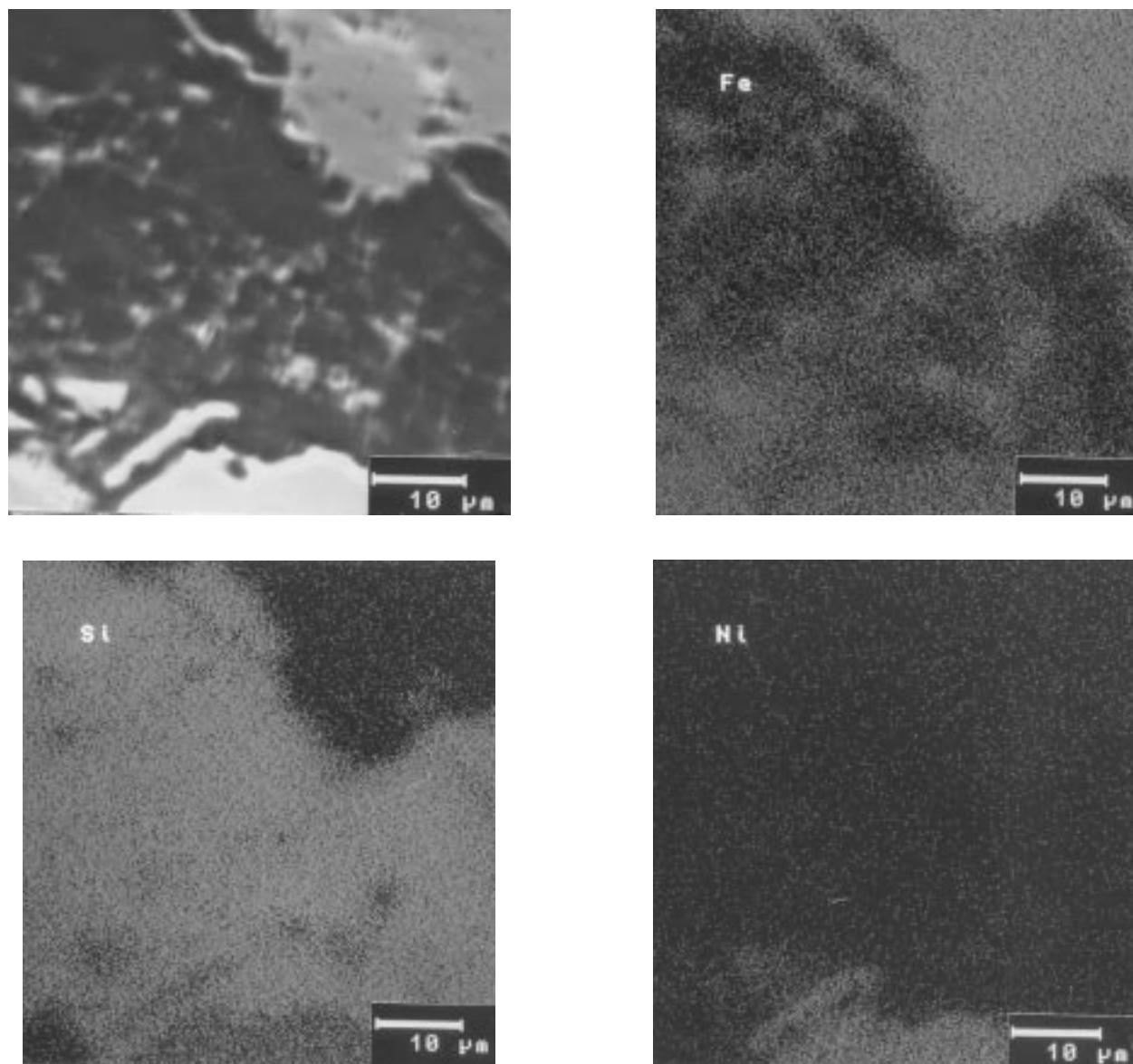


Fig. 3 Secondary electron image of the iron-silicon coating and x-ray mappings for iron, silicon, and nickel

MW depending on energy demand, through the night. After this time of exposure to the combustion gases, when the plant was shut down for repairs, the baffles were dismantled and specimens were taken and mounted in bakelite for observation in an SEM, and the corrosion products were identified using x-ray diffraction (XRD) techniques.

3. Results and Discussion

After 13 months of exposure, the 304 baffles were completely destroyed by corrosion, while the carbon steel baffle coated with Fe75Si-Ni20Cr was intact. No damage could be seen on the coated carbon steel baffle apart from some bending, a result of its poor mechanical properties at high temperatures. Generally speaking, the carbon steel baffle coated with Fe75Si-Ni20Cr showed little accumulation of slags, and this was not strongly adherent because when the baffle was dismantled, the

slags came off easily and the baffle became completely clean. This fact, together with the SEM analysis below, shows that the vanadic slag did not wet the silicon-rich coating and that the silicon itself did not have significant reaction in the melt (Ref 16).

Samples were taken from these plates for metallographic preparation and for analysis in an SEM. Figure 2 shows a cross section of one of these samples with the base metal and the coating together with the energy dispersive x-ray (EDX) spec-

Table 2 Chemical analysis of the coatings

Coating	Elements, wt%					
	Cr	Ni	Fe	Si	C	Mn
Ni20Cr	20	78.5	...	1.5
Fe75Si	26.1	73	0.24	0.55

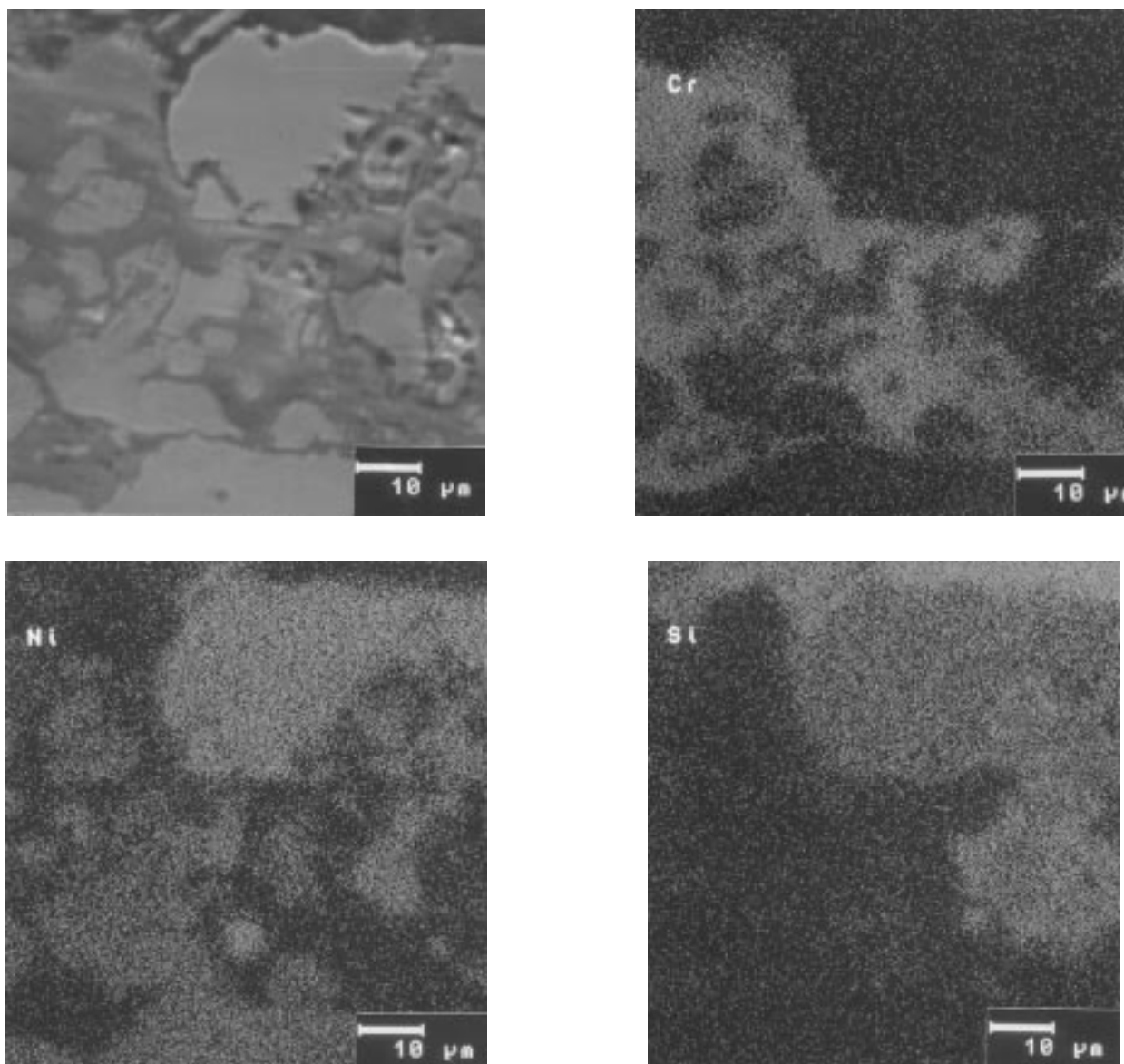


Fig. 4 Secondary electron image of the Ni20Cr coating and x-ray mappings for chromium, nickel, iron, and silicon

tra for different zones of the coating. The marked zones correspond to: (A) an external layer formed mainly with oxidation products and vanadium compounds, (B) iron-silicon coating, (C) Ni20Cr coating whose EDX spectrum shows the presence of iron and silicon, (D) a base metal zone rich in nickel, which probably comes from the Ni20Cr coating, (E) an internal oxidized layer formed with iron oxides, and (F) base metal.

The main compounds identified by XRD were SiO_2 , FeO , FeVO_4 , AlVO_4 , and FeS_2 . The aluminum probably comes from the external sealer used to seal the pores before exposure.

Figure 3 shows a magnification of iron-silicon coating together with the elemental mapping for iron, silicon, and nickel. In the as-deposited state, the coating was brittle and very porous and a metallographic specimen could not be prepared until after exposure to high-temperature conditions. Figure 3 also shows the presence of iron and silicon alloyed with nickel particles from the Ni20Cr coating.

This is more evident in Fig. 4, which shows the structure of the Ni20Cr coating after 13 months. The x-ray mappings show that silicon diffused throughout the nickel particles, but it was stopped by the presence of chromium, which acted as a barrier against the diffusion of silicon. On the contrary, iron, which comes from the base metal, diffused through both nickel and chromium. However there is much more iron associated with the nickel particles than with the chromium, perhaps because diffusion of iron in chromium is three orders of magnitude lower than iron in nickel (Ref 23). Nickel also diffused toward the base metal forming a nickel-rich zone, but chromium did not, even though, according to radioactive tracer diffusion data for pure metals (Ref 23), the diffusion coefficients of chromium and nickel in iron are almost the same.

According to Longa and Takemoto (Ref 24), during the thermal spray deposition of nickel-chromium coatings in air, part of the Cr_2O_3 formed during oxidation of chromium is trapped

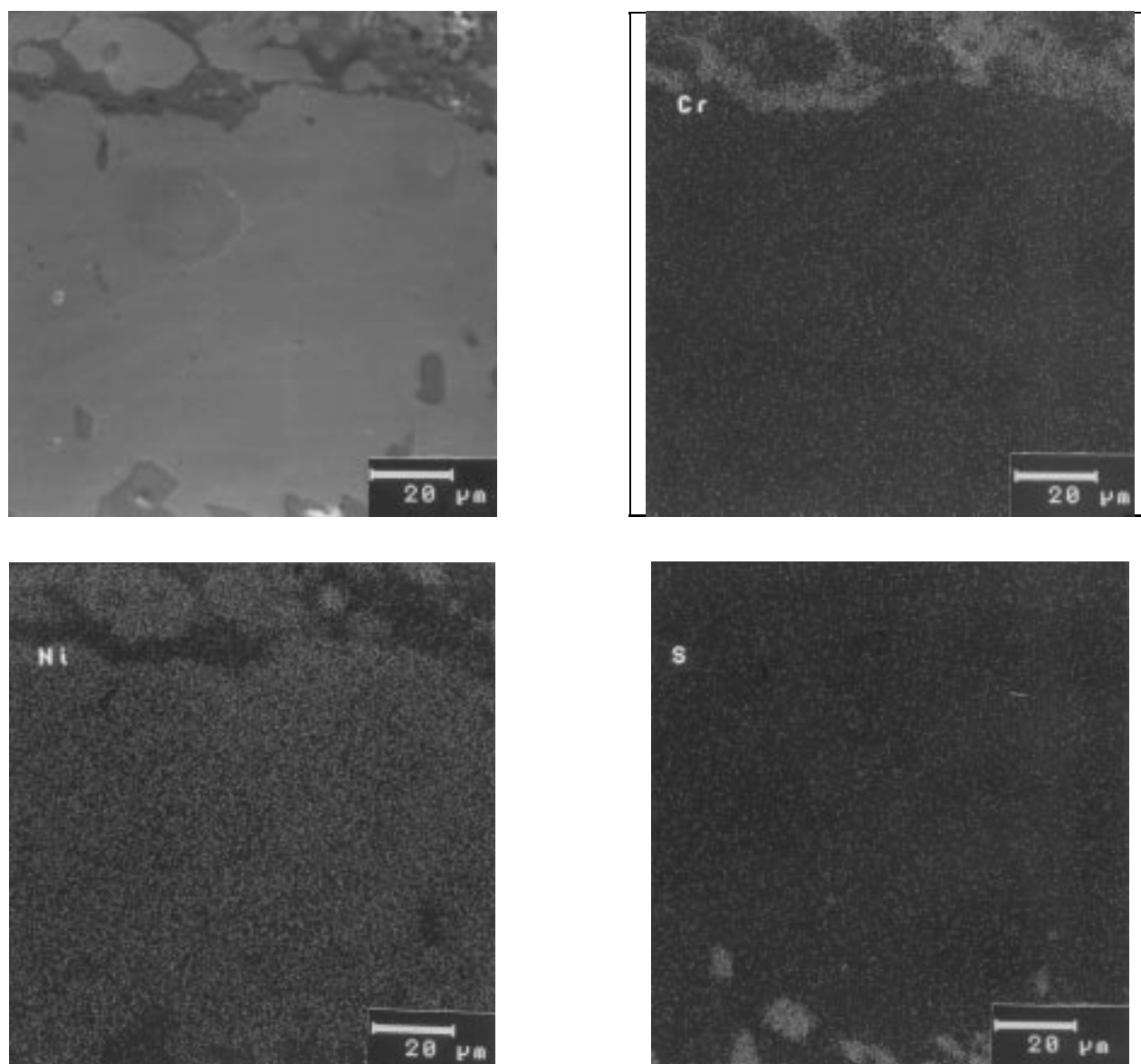


Fig. 5 Secondary electron image of the nickel-rich zone and its corresponding x-ray mappings for chromium, nickel, iron, and sulfur

in the coating, providing an even higher oxidation resistance than the coatings applied in inert environments. The presence of trapped Cr_2O_3 protects the coating from further oxidation. The oxidation of chromium could have acted as a barrier against diffusion of chromium toward the base metal.

Semiquantitative analysis done by EDX on the Ni20Cr coating showed that the amount of chromium remained unaltered, but the amount of nickel was lowered from 80 to 20 wt%, indicating that the remaining 60% diffused toward the base metal, and the iron content of the coating was 54%. The amount of silicon depended on the chromium concentration next to the nickel particles.

Figure 5 shows an aspect of the nickel-rich base metal with an average thickness of about 100 μm . In places with lower contents of chromium in the coating base metal interface, the thickness was up to 150 μm . In this zone the content of nickel was around 14%, and also some islands of iron oxides can be seen at either grain boundaries or material defects. These de-

fects, together with the coating porosity could have made diffusion of oxygen easier and could have reacted with the base metal elements to form oxides.

After the nickel-rich zone, an internal oxidized layer was detected with an average thickness of 200 to 250 μm (Fig. 2e). The layer is porous, and it has mainly iron oxides. The presence of iron sulfides was detected only along the interface between these two layers (Fig. 5 and 6). According to this it can be said that the nickel-rich zone was resistant to sulfur attack, because the presence of sulfides started at the point where the nickel diffused. The sulfur species diffused toward the base metal to react with manganese and to form manganese sulfides at the grain boundaries (Fig. 7).

Evidence suggests that the coating system used here was highly protective, but the high porosity of the initial iron-silicon coating together with the rather high temperatures (above 900 $^\circ\text{C}$) and the boiler operating time (13 months) promoted the beginning of the protective system degrada-

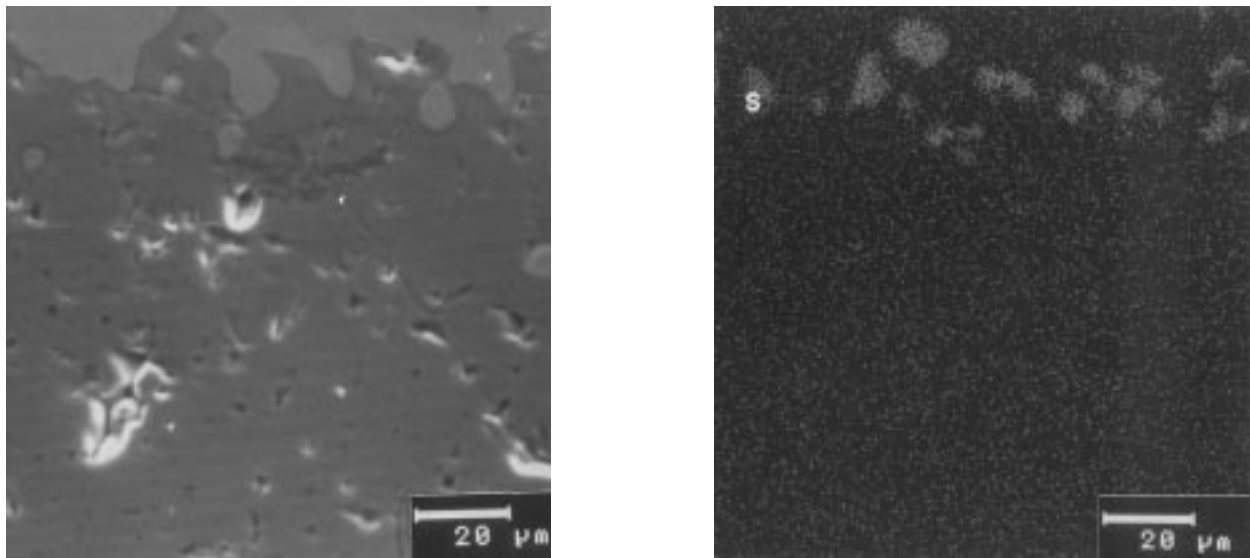


Fig. 6 Secondary electron image of the interface between the nickel-rich zone and the internal oxidized layer and x-ray mappings for sulfur

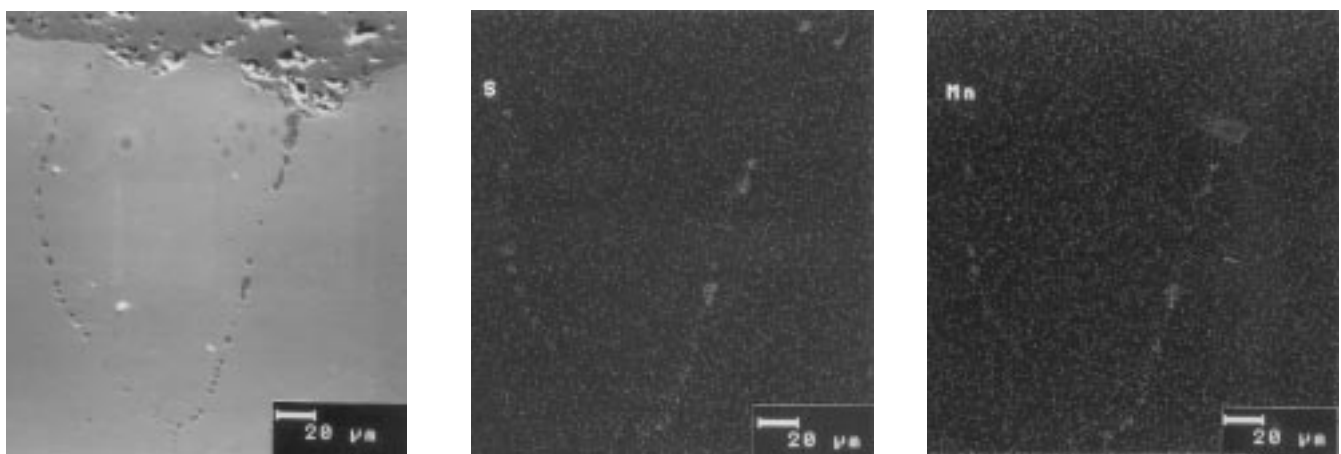


Fig. 7 Secondary electron image of the internal oxidized layer/base metal interface, showing sulfidation along the grain boundaries together with the x-ray mappings for sulfur and manganese

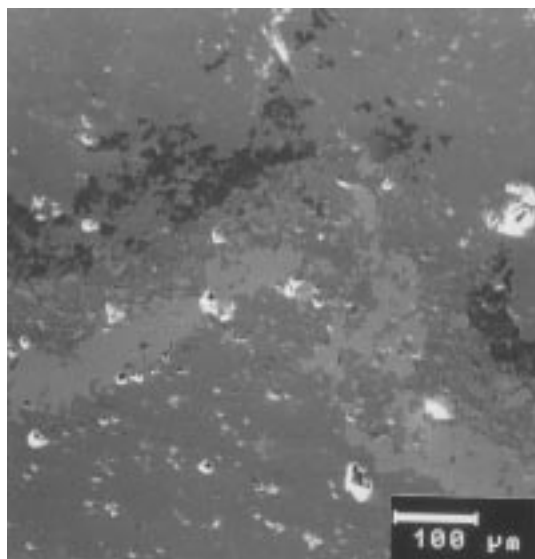


Fig. 8 Secondary electron image of the fractured coating and the nickel-rich layer together with the x-ray mappings for silicon

tion. It is evident that the compactness of the iron-silicon coating due to phase transformation was achieved in a short period of time, because neither vanadium nor sulfur was detected throughout the coating. This was due to the aluminum sealer layer.

Due to the concentration gradient of elements between the coating system and the base metal, nickel diffused, forming a nickel-rich layer reaching a “steady state” (20% Ni in the coating and 14% Ni in the base metal next to coating). Similarly, iron from the base metal diffused toward the NiCr coating. Diffusion of chromium was not achieved for the reasons given above.

The achievement of an internally oxidized layer can be due to the diffusion of oxygen through the pores and imperfections of the coating and the base metal. Stresses induced in the formation of this layer deformed and fractured the coating system and the nickel-rich layer encouraging the penetration of oxidizing agent (Fig. 8). Later, this path for the oxidizing agent made easier the oxidation of the interface between the nickel-rich layer and the base metal.

The analyzed samples did not show evidence of sulfidation of the coating, except in the interfaces of the internal oxidized layer and the base metal. This suggests that penetration of sulfur occurred through points where the coating was deformed and fractured, and then the sulfur diffused through the porous oxidized layer (Fig. 8).

Oxidation of the base metal can be avoided by lowering the porosity of the coating and/or alloying the substrate with chromium or nickel to minimize the diffusion of elements from the coating. The porosity can be lowered if the iron-silicon coating is applied using other techniques such as plasma or high-velocity oxygen-fuel (HVOF) thermal spray. Even when a degradation of the coating system was observed due to the diffusion of oxygen, it can be said that the double layer Fe75Si-Ni20Cr coating system has a high corrosion resistance for temperatures above 900 °C.

4. Conclusions

The double-layer Fe75Si-Ni20Cr coating system is highly resistant to high-temperature corrosion. Its performance was proved when it was applied on carbon steel plates exposed to temperatures above 900 °C in a highly corrosive environment, together with type 304 plates, which showed catastrophic corrosion rates. After 13 months, it was observed that the protective system started to degrade due to diffusion of oxygen through pores and imperfections in the coating. This diffusion of oxygen resulted in an internal layer of iron oxides between the base metal and a nickel-rich layer in the base metal. The quality of the iron-silicon coating can be enhanced by applying it with a plasma spray or HVOF technique.

Acknowledgment

This work was carried out under the IIE project No. 3231. The authors would like to thank Mrs. A. Wong-Moreno and Dr. D. Lopez-Lopez for their invaluable comments on this work.

References

1. F.H. Stott, *Mater. Sci. Technol.*, Vol 5 (No. 8), 1989, p 734-740
2. F. Fitzer and J. Schlichting, Coatings Containing Chromium, Aluminum, and Silicon for High Temperature Alloys, *High Temperature Corrosion*, 2-6 March 1981 (San Diego, CA), R.A. Rapp, Ed., National Association of Corrosion Engineers, p 604-614
3. A. Atkinson and J.W. Gardner, *Corros. Sci.*, Vol 21, 1981, p 49-58
4. A. Atkinson, *Corros. Sci.*, Vol 22 (No. 2), 1982, p 87-102
5. T. Adachi and G.H. Meier, *Oxid. Met.*, Vol 27 (No. 5/6), 1987, p 347-366
6. H.E. Evans, D.A. Hilton, R.A. Holm, and S.J. Webster, *Oxid. Met.*, Vol 19 (No. 1/2), 1983, p 1-18
7. J. Robertson and M.I. Manning, *Mater. Sci. Technol.*, Vol 5 (No. 8), 1989, p 741-753
8. S.R.J. Saunders and J.R. Nicholls, *Mater. Sci. Technol.*, Vol 5 (No. 8), 1989, p 780-798

9. J. Porcayo-Calderon, S. D'Granda, and L. Martinez, *CORROSION*, 95, paper 466, NACE International, 1995
10. A.A. Ansari, S.R.J. Saunders, M.J. Bennett, A.T. Tuson, F. Ayres, and W.M. Steen, *Mater. Sci. Eng.*, Vol 88, 1987, p 135-142
11. G. Southwell, S. MacAlpine, and D.J. Young, *Mater. Sci. Eng.*, Vol 88, 1987, p 81-87
12. Zh.A. Mrochek, B.A. Eizner, and I.A. Ivanov, *CORROSION*, 91, paper 452, NACE International, 1991
13. M.P. Hill, *Mater. Sci. Technol.*, Vol 5 (No. 8), 1989, p 835-840
14. H. Van Amerongen, Structure and Properties of Silicide Based Diffusion Coatings, *High Temperature Alloys for Gas Turbines*, D. Coutouradis, P. Felix, H. Fischmeister, L. Habraken, Y. Lindblom, and M.O. Speidel, Ed., Applied Science, 1978, p 209-224
15. H. Caillet, F. Ayedi, A. Galerie, and J. Besson. Preparation and Oxidation of Zirconium Silicides Coatings on Zirconium, *Materials and Coatings to Resist High Temperature Corrosion*, D.R. Holmes and A. Rahmel, Ed., Applied Science, 1978, p 387-398
16. P. Elliot and T.J. Taylor, Some Aspects of Silicon Coatings under Vanadic Attack, *Materials and Coatings to Resist High Temperature Corrosion*, D.R. Holmes and A. Rahmel, Ed., Applied Science, 1978, p 353-366
17. G. Wahl and B. Furst, "Preparation of Lasers Enriched in Silicon by Chemical Vapor Deposition, *Materials and Coatings to Resist High Temperature Corrosion*, D.R. Holmes and A. Rahmel, Ed., Applied Science, 1978, p 333-351
18. H. Murakami, T. Yoshida, and K. Akashi, *Adv. Ceram. Mater.*, Vol 3 (No. 4), 1988, p 423-426
19. Y. Hirohata, N. Kobayashi, S. Maeda, K. Nakamura, M. Mohri, K. Watanabe, and T. Yamashina, *Thin Solid Films*, Vol 63, 1979, p 237-242
20. A. Wong-Moreno, Y. Mujica-Martinez, and L. Martinez, *CORROSION*, 94, paper 185, NACE International, 1994
21. D. Lopez-Lopez, A. Wong-Moreno, and L. Martinez, *CORROSION*, 95, paper 464, NACE International, 1995
22. M. Vita-Peralta, E. Manzanares, and M. Ley-Koo, Study in progress, Instituto de Investigaciones Electricas, Cuernavaca, Morelos, Mexico
23. R.C. Weast, *Handbook of Chemistry and Physics*, CRC Press, 1986-1987, p F46-F51
24. Y. Longa and M. Takemoto, *Corros. Sci.*, Vol 50 (No. 11), 1994, p 827-837